water

MDPI

Article

Cyanide Removal and Recovery by Electrochemical Crystallization Process

Natacha Martin [1], Vinh Ya [1,2], Vincenzo Naddeo [3], Kwang-Ho Choo [4] and Chi-Wang Li [1,*]

[1] Department of Water Resources and Environmental Engineering, Tamkang University, New Taipei City 25137, Taiwan; natacha.martind@gmail.com (N.M.); vinhy@dlu.edu.vn (V.Y.)
[2] Faculty of Chemistry and Environment, Dalat University, Dalat P8, Vietnam
[3] Department of Civil Engineering, SEED Sanitary Environmental Engineering Division, University of Salerno, Via Ponte don Melillo 1, 84084 Fisciano, Italy; vnaddeo@unisa.it
[4] Department of Environmental Engineering, Kyungpook National University, 80 Daehak-ro, Buk-gu, Daegu 702-701, Korea; chookh@knu.ac.kr
* Correspondence: chiwang@mail.tku.edu.tw; Tel.: +886-2-26239343; Fax: +886-2-26209651

Abstract: Alkaline chlorination, an efficient but high chemical cost process, is commonly employed for cyanide (CN^-) removal from CN-rich wastewater streams. CN^- removal and recovery through the precipitation of Prussian Blue ($Fe_4^{III}[Fe^{II}(CN)_6]_3$, PB) or Turnbull's Blue ($Fe_3^{II}[Fe^{III}(CN)_6]_2$, TB) were realized using iron salts, leading to a cost-effective and sustainable process producing a valuable recovery product. However, the precipitation of PB and TB is highly affected by pH and dissolved oxygen (DO). CN^- removal and recovery from CN-containing water by crystallization of PB and/or TB were investigated using dissolved iron that was electrochemically generated from a sacrificial iron anode under various pH values, initial CN^- levels (10 to100 mg/L) and DO levels (aeration, mechanical mixing, and N_2 purging). It was shown that the complexation of CN^- with Fe ions prevented the vaporization of HCN under acidic pH. At pH of 7 and initial CN^- concentration of 10 mg/L, CN^- removal efficiency increases linearly with increasing Fe:CN^- molar ratios, reaching 80% at the Fe:CN^- molar ratio of 5. A clear blue precipitate was observed between the pH range of 5–7. CN^- removal increases with increasing initial CN^- concentration, resulting in residual CN^- concentrations of 8, 7.5 and 12 mg/L in the effluent with the Fe:CN^- molar ratio of 0.8 for initial concentrations of 10, 50 and 100 mg CN^-/L, respectively. A polishing treatment with H_2O_2 oxidation was employed to lower the residual CN^- concentration to meet the discharge limit of <1 mg CN^-/L.

Keywords: cyanide removal; crystallization; prussian blue; iron hexacyanoferrate

Citation: Martin, N.; Ya, V.; Naddeo, V.; Choo, K.-H.; Li, C.-W. Cyanide Removal and Recovery by Electrochemical Crystallization Process. *Water* **2021**, *13*, 2704. https://doi.org/10.3390/w13192704

Received: 13 August 2021
Accepted: 24 September 2021
Published: 29 September 2021

1. Introduction

CN^- is a common contaminant encountered in the wastewater streams from mining and electroplating processes. As an example, China has encountered high environmental pollution due to the discharge of cyanide from gold mining operations and, therefore, has set a strict discharge limit to 0.5 mg/L for sewers [1]. Cyanide is usually treated with an oxidation process under alkaline conditions using oxidants, such as hypochlorite [2]. Although alkaline chlorination is an efficient process for the removal of cyanide to reach the discharge limit of 1 mg CN^-/L in Taiwan, the process is highly pH-dependent and associated with high chemical costs [3,4].

Few studies have investigated the removal and recovery of cyanide as valuable products using chemical precipitation with iron salt through the precipitation of Prussian Blue ($Fe_4^{III}[Fe^{II}(CN)_6]_3$, PB) and/or Turnull's Blue ($Fe_3^{II}[Fe^{III}(CN)_6]_2$, TB) [5–7]. The summary of these studies is shown in Table 1. Recovering cyanide as PB and TB has specific advantages, as these materials can be utilized in the production of coatings and ink colorants [8]. Yu et al. (2016) proposed a two-step reaction for the precipitation of PB which was dependent on the Fe:CN^- molar ratio. As indicated in Equation (1),

ferrous ions first complex with CN^- to form $Fe^{II}(CN)_6{}^{4-}$. Once extra ferrous is added, the precipitation of $Fe^{II}{}_2Fe^{II}(CN)_6$ immobilizes and removes CN^- from the solution with a Fe(II):CN^- molar ratio of 0.5, as illustrated in Equation (2). With dissolved oxygen (DO), $Fe^{II}{}_2Fe^{II}(CN)_6$ is oxidized to form PB as indicated in Equation (3), releasing ferrous. Based on the stoichiometric ratio, the overall Fe:CN^- molar ratio is 7/18, i.e., 0.39, for the precipitation of pure Prussian Blue.

$$Fe^{2+} + 6CN^- \rightarrow Fe^{II}(CN)_6^{4-} \quad (1)$$

$$2Fe^{2+} + FeCN_6^{4-} \rightarrow Fe_2^{II}Fe^{II}(CN)_6 \quad (2)$$

$$3Fe_2^{II}Fe^{II}(CN)_6 + O_2 + 4H^+ \rightarrow 2Fe^{2+} + Fe_4^{III}[Fe^{II}(CN)_6]_3 + 2H_2O \quad (3)$$

However, these authors reported only 70% of CN^- removal at the Fe:CN^- molar ratio of 1 using ferrous sulfate for treating coking wastewater at pH 9 due to the competition of cyanide with other pollutants [7]. Adams (1992) concluded that 99% of CN^- removal from synthetic wastewater used ferrous sulfate at the Fe:CN^- molar ratio of 0.5, O_2 concentration of 6.5 mg/L and the optimal pH range of 5.5 to 6.5. The author reported increasing DO level increased $Fe^{III}(CN)_6{}^{3-}$ and $Fe^{II}(CN)_6{}^{4-}$ complexation, leading to the decrease of CN^- recovery efficiency. However, vaporization of HCN under acidic pH range has not been assessed in those studies. In contrast, Mamelkina et al. [9] compared chemical coagulation (CC) using ferric salts and electrochemical coagulation (EC) using iron anode for CN^- removal at pH 12. CN^- removal was very inefficient by CC (only 15%), while a complete removal of CN^- was achieved by EC. At pH > 8.5, the negative surface charge of ferric hydroxide [10] makes the adsorption of negatively charged cyanide ions onto ferric hydroxides less efficient. Moreover, non-charged HCN dominating at pH < 9.2 is not expected to be removed by coagulation. Mamelkina et al. [9] indicated that formation and precipitation of PB with the electrogenerated ferrous ions in EC could be responsible for CN^- removal; it was reported that 92% of CN^- removal was achieved at the Fe:CN^- molar ratio of 0.9. The ratio is much higher than the value based on the precipitation of PB, i.e., 0.39. It could be related to the high alkaline condition of pH 12 in the study, where competition between the precipitation of PB and ferrous hydroxides might occur. It is well-known that ferrous can be oxidized easily by DO at elevated pH [11,12]. The conversion of ferrous to ferric followed by precipitation of ferric to ferric hydroxides consumes additional ferrous. By using EC, Moussavi et al. [13] showed that CN^- removal efficiency increased with aeration due to the adsorption/complexation of CN^- with iron hydroxide and increasing Fe:CN^- molar ratio at a pH of 11.5. The volume of sludge produced increased under aeration condition, increasing the surface area for adsorption/complexation.

Table 1. Details of the conditions for the removal of CN^- using Chemical Precipitation (CP), CC or EC. C_i: Initial CN^- concentration; C_f: effluent CN^- concentration; R: removal.

Authors	Process	C_i–C_f, mg/L	Fe:CN^- Molar Ratio	pH	R, %
Yu et al. [7]	CP	53.6–16.1	1.0	9	70
Adams et al. [6]	CP	265–2.6	0.5	5.5–6.5	99
Mamelkina et al. [9]	CC	100–85	46	12	15
	EC	100–0.8	0.9	12	92
Zhao et al. [14]	EC	75–39.9	1.7	4	47
Moussavi et al. [13]	EC	300–39	5.2	11.5	87

Electrochemical crystallization of PB has more advantages than chemical precipitation, such as easy operation, no need for chemical additions and low-costs [15]. Moreover, the EC process might be a superior process to alkaline chlorination because of its low chemical cost and its ability to recover valuable sludge. The iron species, affected by DO and pH conditions, have a profound impact on the CN^- removal mechanisms. Further

investigations of the mechanism and its optimal conditions need to be done. Initial CN^- concentration, which was mostly investigated at the value of 100 mg/L or more in the previous studies [9,13,16], could affect PB precipitation. Thus, the objectives of the study are to investigate the effect of Fe dosage, pH, initial CN^- concentration and DO level on the removal and recovery of cyanide as valuable products using EC with a sacrificial iron anode from CN-containing synthetic wastewater. The formation of TB and/or PB was assessed by chemical equilibrium models and solid analysis.

2. Materials and Methods

2.1. Cyanide-Containing Water

All chemicals were of reagent grade. Stock solution containing 1 g CN^-/L was prepared by dissolving reagent grade potassium cyanide (KCN, Acros Organics, Merelbeke, Belgium) in deionized water, and the pH of the stock solution was adjusted to 11. Synthetic CN-containing water was prepared by diluting the stock solution to various concentrations (10, 50 and 100 mg/L). The conductivity of the prepared water was adjusted to 4 mS/cm by adding NaCl.

2.2. Experimental Setup

A 2-L Pyrex glass, containing 1 L of CN^- solution, was used as the reactor as shown in Figure 1. Anode and cathode were made of iron plates with the same dimension of 25 cm × 5 cm × 0.3 cm and a spacing of 1 cm between the two electrodes. Part of the electrode area was covered with an insulation tape to obtain the working electrode area of 41 cm^2. The experiments were conducted in constant current mode using a direct current power supply (GPS-3030DD, Taiwan) with a fixed current intensity of 1 A, corresponding to a current density of 24.4 mA/cm^2. The reactor was capped and the gas phase HCN was trapped by directing the air flow from the reactor to a 1-L NaOH trapping solution (0.5 M) where HCN was converted to CN^-. Samples were collected from the reactor and the trapping solution to estimate HCN vaporization during the experiment. Three DO levels were created by mixing the reactor with a magnetic stirrer (initial DO = 5.1 mg O_2/L) (Cemarec Stirring Hot Plates, MA, USA) and purged with either N_2 gas (initial DO = 1.0 mg O_2/L) or air (initial DO = 8.3 mg O_2/L) at the flow rate of 2.5 L/min. DO levels were measured with a DO meter (DO-5509, Lutron Electronic Enterprise, Taipei, Taiwan). The solution pH was maintained at the desired values throughout the reaction by dosing 0.1 M H_2SO_4 solution through an automatic pH controller (PC3200, Suntex Instruments Co., Ltd. Kaohsiung, Taiwan). The solution was circulated by a pump (120 mL/min) to the pH sensing unit installed above the reactor to avoid the effect of electric field on the pH electrode.

Samples were collected at various theoretical Fe:CN^- molar ratios based on Faraday's law, filtered with 0.45-μm membrane filters and analyzed for CN^-, Fe(II) and total dissolved Fe concentrations. CN^- removal efficiency was plotted as function of the experimental Fe:CN^- molar ratio instead of the theoretical Fe:CN^- molar ratio. Triplicate experiments were performed, and the mean and one standard deviation were reported.

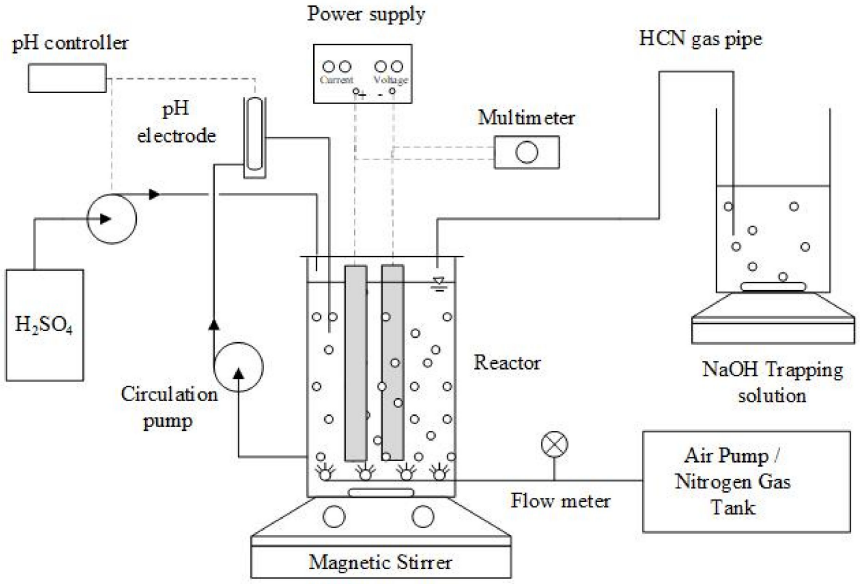

Figure 1. Scheme of the experimental setup.

2.3. Analytical Methods

Total cyanide concentration was analyzed colorimetrically at wavelength of 578 nm (UV-visible spectrophotometer, Varian Cary 50, Walnut Creek, CA, United States) using chloramine-T solution and pyridine-barbituric acid reagent following the Standard Methods (4500-CN^- E) [17]. The concentration range for the standard curve was from 0 to 0.20 mg CN^-/L.

Dissolved Fe concentration analysis was carried out by using an Inductively Coupled Plasma mass spectrometry (ICP-OES 5110, Agilent Technologies, Santa Clara, CA, United States). Ferrous concentration was determined colorimetrically at a wavelength of 510 nm (T70+ UV-Vis Spectrophotometer, PG Instruments Limited, Lutterworth, UK) using a phenanthroline indicator as described in the Standard Methods (3500-Fe B) [17]. The range of concentration for the standard curve was from 0 to 10 mg Fe/L. Ferric concentration was determined by subtracting Fe(II) ions' concentration from the dissolved Fe concentration.

Solid sample was collected by centrifuging, then dried in a vacuum dryer. The crystal structure analysis was analyzed using an X-ray diffraction system (XRD, AXS D8 ADVANCE, Bruker, Billerica, MA, USA). Particles were identified by comparing the diffraction pattern with the crystallography open database [18]. Scanning electron microscope coupled with an energy dispersive X-ray detector system (SEM-EDX, JSM-7600F, JEOL Ltd., Tokyo, Japan) was used for morphology and elemental composition analysis of the solid samples.

3. Results and Discussion

3.1. Chemical Equilibrium Modeling

Chemical equilibrium modeling using a commercial chemical equilibrium software, MINEQL+, was first performed with the condition set at the temperature of 25 °C and the initial cyanide concentration of 10 mg/L to reveal the effects of pH and Fe:CN^- molar ratio on the formation of the primary $Fe^{II}(CN)_6^{4-}$ and $Fe^{III}(CN)_6^{3-}$ complexes involved in the precipitation of PB and TB, respectively.

Figure 2A shows the distribution of CN^- in the $Fe^{II}(CN)_6^{4-}$ complex as a function of Fe(II):CN^- molar ratio. The complex forms at pH of >6.5 and the percentage of CN^- in the complex reaches the plateau of 98% at pH 8 for the Fe(II):CN^- molar ratio of >0.2. According to the modeling, the excess ferrous precipitates as ferrous hydroxide at pH of >8 (see Supplementary Figure S1). Figure 2B shows the distribution of CN^- as a function of Fe(III):CN^- molar ratio and pH for the formation of $Fe^{III}(CN)_6^{3-}$. $Fe^{III}(CN)_6^{3-}$ starts forming at pH of >7 at the Fe(III):CN^- molar ratio >0.2. According to the modeling, the excess iron precipitates as ferric hydroxides (see Supplementary Figure S2). At pH > 10,

the $Fe(OH)_4^-$ complex forms. Based on the modeling result, $Fe^{II}(CN)_6^{4-}$ complex forms at 6.5 < pH < 10.5, and Fe(II):CN^- molar ratio of >0.2. $Fe^{III}(CN)_6^{3-}$ complex forms at the pH range of 7 to 9 and the Fe(III):CN^- molar ratio of >0.2.

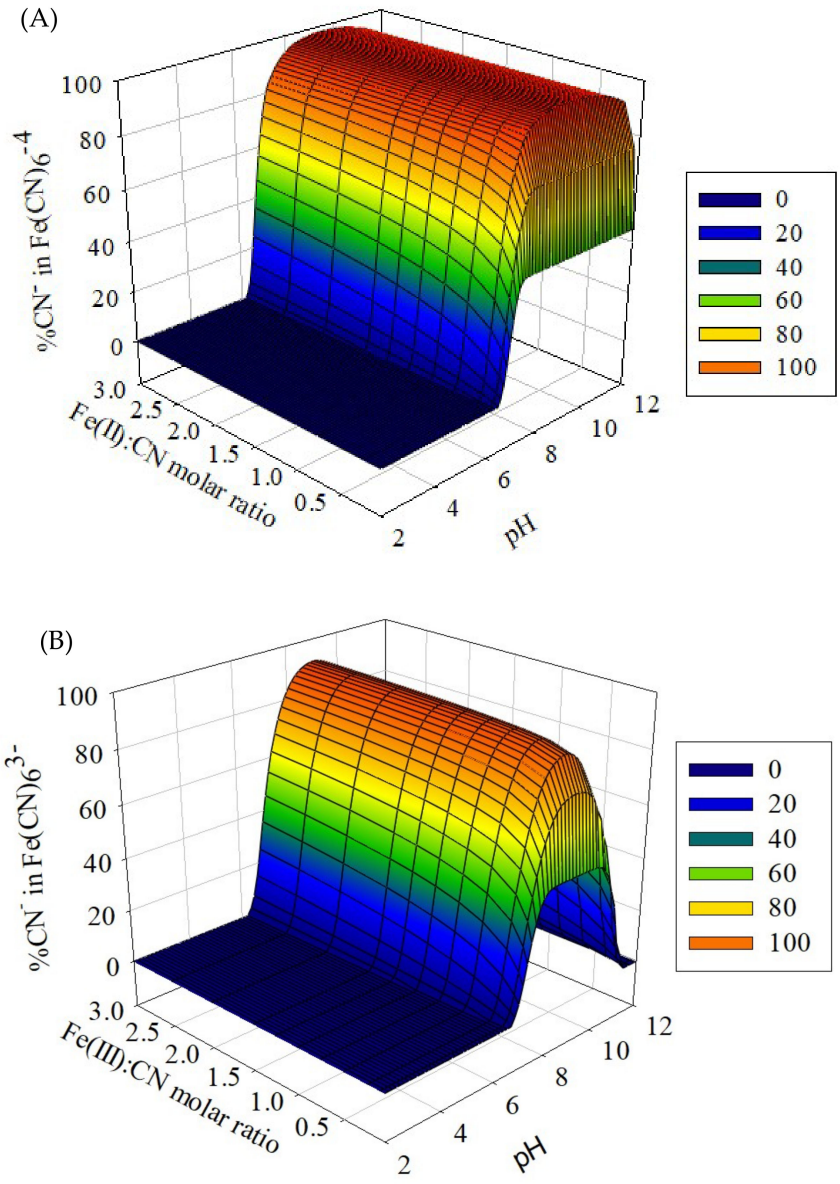

Figure 2. Percentage of (**A**) CN^- in $Fe^{II}(CN)_6^{4-}$ and (**B**) CN^- in $Fe^{III}(CN)_6^{3-}$ as a function of Fe:CN^- molar ratio and pH modeled by MINEQL+. Fixed CN^- concentration of 10 mg/L. Temperature of 25 °C.

The effects of pH and initial CN^- concentration on the formation of PB were modeled under the fixed O_2 concentration of 5 mg O_2/L, the temperature of 25 °C and the fixed Fe:CN^- molar ratio of 0.5. As shown in Figure 3, 99% of CN^- was removed in the form of PB at pH < 7 and initial CN^- concentration of >50 mg/L. When pH increased, the percentage of cyanide in PB decreased. Moreover, the percentage of CN^- recovered in PB increased with initial CN^- concentration. At initial CN^- concentration of 10 mg/L, the percentage of CN^- in PB does not exceed 25%; on the contrary, the maximum cyanide percentage in PB is 85% at the initial CN^- concentration of 50 mg/L. Even when the cyanide percentage is at the maximum, the dissolved CN^- concentration in solution will not reach the discharge standards (1 mg CN^-/L) into the environment, and no polishing treatment process would be necessary. According to the modeling, the excess of iron

precipitates as ferric hydroxide when Fe:CN^- molar ratio >0.39 (theoretical Fe:CN^- molar ratio for the formation of PB), affecting the purity of PB. In conclusion, the equilibrium modeling showed cyanide can be formed as PB at pH of 7 or less and Fe:CN^- molar ratio of 0.5 to recover the highest percentage of cyanide. Increasing the initial CN^- concentration increased the recovery rate.

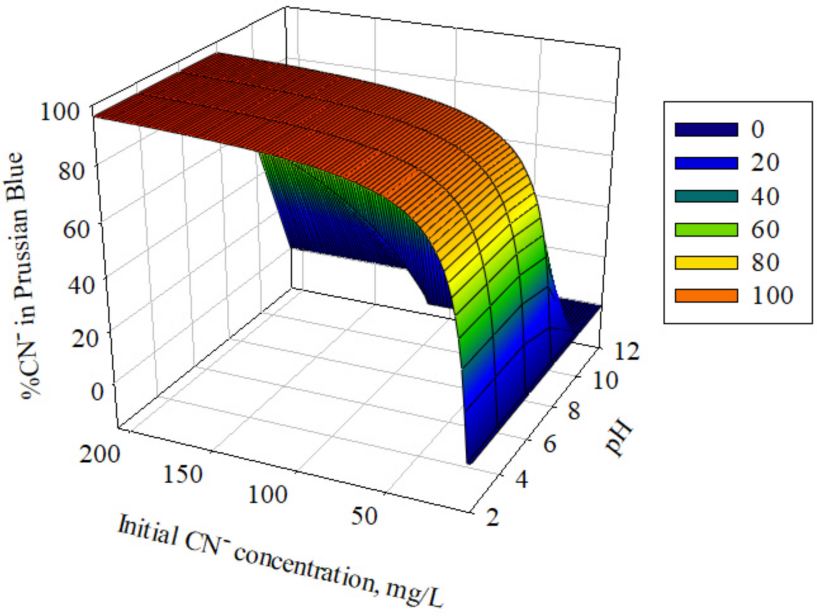

Figure 3. Percentage of CN^- in PB and concentration of residual CN^- as function of initial CN^- concentration and pH at Fe:CN^- molar ratio of 0.5 by MINEQL+. Fixed DO of 5.0 mg O_2/L. Temperature of 25 °C.

3.2. Effects of pH on HCN Vaporization

Since the formation of PB is favored under acidic to neutral pH range and it is known that HCN is the dominant specie at pH < 9.2, the effects of pH on HCN vaporization were investigated for systems with or without current applied by capturing vaporized HCN in a NaOH trapping solution. Vaporized HCN was completely trapped in the NaOH solution as indicated by the nearly 100% mass balance shown in Figure 4. For an experiment conducted at pH 4, a small percentage (<5%) of CN^- might evaporate through the recirculation system for pH measurement. After 30 min, more than 45% of CN^- vaporized at pH of 4 and 7 in a system without current applied. The amount of HCN vaporized decreased with increasing pH. At pH 11, only 1.3% of CN^- was vaporized. During the electrolytic process, almost no CN^- vaporized as HCN for any pH. Thus, the complexation of FeCN could prevent the HCN vaporization and the electrochemical process using iron sacrificial anode could be operated under any pH values without concerning HCN vaporization.

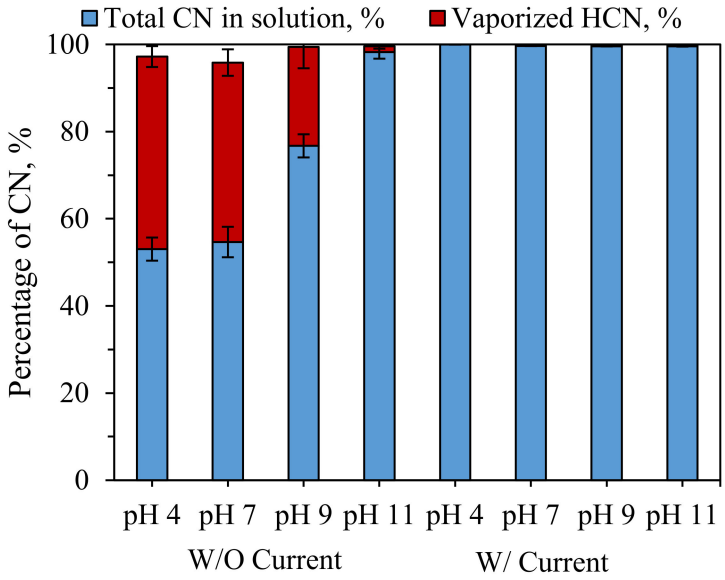

Figure 4. Mass balance of CN^- in the system as a function of various pH values with and without current applied. Initial CN^- concentration of 10 mg/L. Current intensity of 1 A. N_2 purging and mechanical mixing. Reaction time of 30 min.

3.3. Effects of pH

The effect of control pH was investigated in the pH range of 4 to 11 with an initial CN^- concentration of 10 mg/L. As shown in Figure 5A, removal of CN^- increased with pH values from 4 to 7. CN^- removal increased and reached the steady value of 90% and the theoretical Fe:CN^- molar ratio > 6 at pH values from 7 to 10. At pH of 11, CN^- removal decreased and only 75% of removal was achieved. As predicted in the modeling, CN^- recovery decreased when pH exceeds 7 (see Figure 3). Nevertheless, the dissolved Fe concentration decreased when pH > 7 as shown in Figure 5B, i.e., the excess of Fe precipitates as ferrous hydroxide. The increasing of CN^- removal for higher Fe:CN^- molar ratio is due to CN^- adsorption on iron hydroxide at pH > 7. When pH < 7, the removal of cyanide is mostly attributed to the precipitation of PB. At pH < 7 and the Fe:CN^- molar ratio < 5, the solution has an intense blue color, specific to PB. When pH increased, the color of the solution turned to a dark blue-green color, indicating the presence of ferrous hydroxide. Figure 5C,D showed the diffraction patterns of the precipitates, produced at the theoretical Fe:CN^- molar ratio of 0.8 and pH 5 and 7, respectively, for an initial CN^- concentration of 10 mg/L. The diffraction pattern for the sample collected at pH 5 indicated that PB was near the sole product generated. However, the diffraction pattern of the precipitate produced at pH 7 showed peaks contributed by impurities in the precipitate, matching with the patterns of Prussian Blue and iron oxide. At pH 5, the quality of PB recovered was better than at pH 7 but cyanide removal was lower. With the objective of optimizing the recovery and removal of cyanide, further experiments were conducted at the pH value of 7.

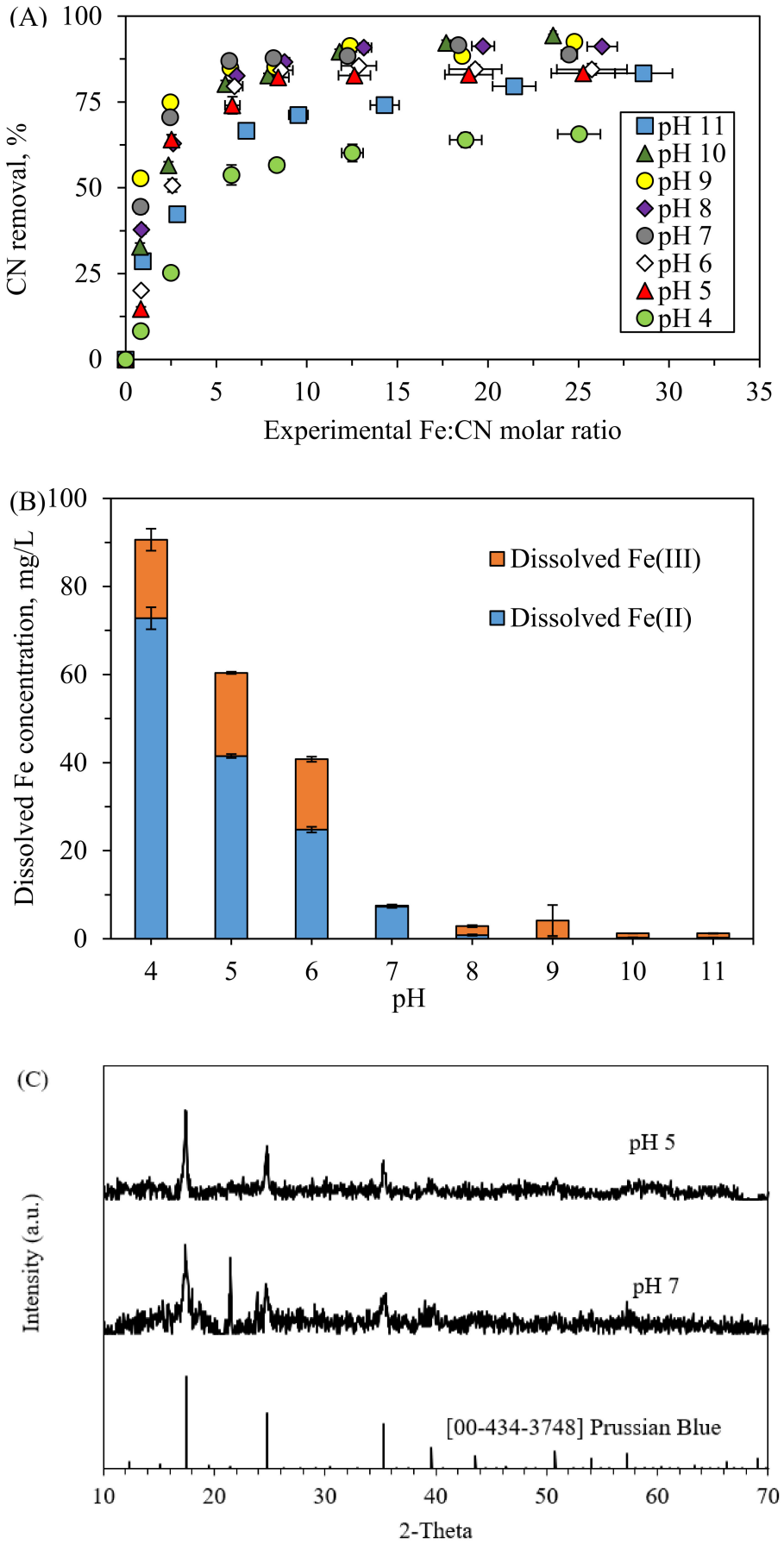

Figure 5. *Cont.*

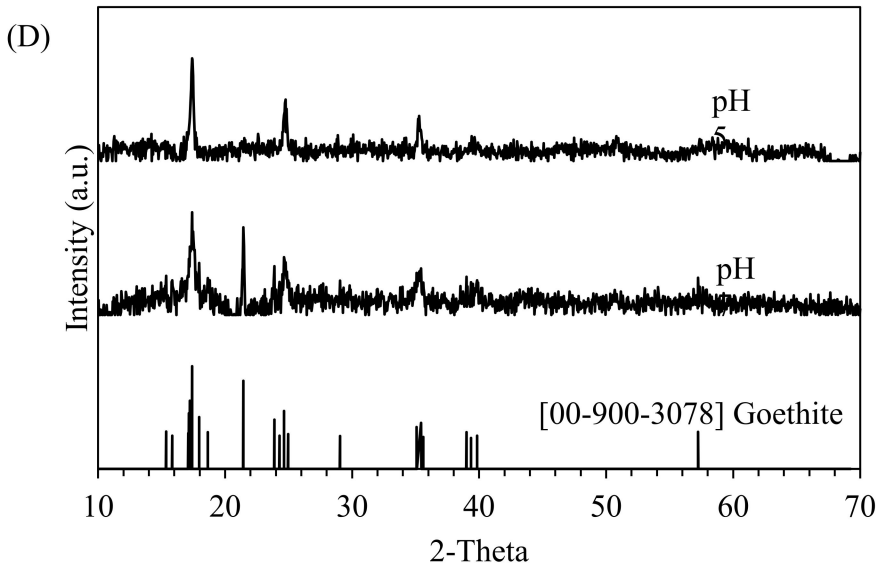

Figure 5. (**A**) CN^- removal as a function of the experimental Fe:CN^- molar ratio for various control pH values. (**B**) Dissolved Fe(II) and Fe(III) concentration as a function of various pH values at the theoretical Fe:CN^- molar ratio of 5.7. (**C**,**D**) XRD powder pattern of precipitate produced at pH 5 and 7 and theoretical Fe:CN^- molar ratio of 0.8. Initial CN^- concentration of 10 mg/L. Current intensity of 1 A. Mechanical mixing.

3.4. Effects of Initial CN^- Concentrations

Various studies investigated CN^- removal by EC at an initial CN^- concentration of 100 mg/L or higher [9,13,16]. In this study, the effect of initial CN^- concentration as low as 10 mg/L was investigated. Figure 6A shows CN^- removal for various initial CN^- concentrations (10, 50 and 100 mg/L) at the control pH of 7. At the initial CN^- concentration of 10 mg/L, CN^- removal increased with increasing Fe:CN^- molar ratio and reached 90%, i.e., 1 mg/L for the residual CN^- in the treated water, at the experimental molar ratio of 5. At the initial CN^- concentrations of 50 and 100 mg/L, CN^- removal reached the steady value of 97% at the experimental Fe:CN^- molar ratio of around 1.2, corresponding to the final CN^- concentration of 1.5 and 3 mg/L, respectively. CN^- removal of 59% and 68% were achieved at the Fe:CN^- molar ratio of 0.5 for both initial CN^- concentration of 50 and 100 mg/L, respectively. Cyanide removal reaches a background concentration of around 10 mg/L, i.e., the solubility of solids produced, irrespective of initial cyanide concentration. As a result, the cyanide removal increases with the initial cyanide concentration. At initial CN^- concentrations of 50 and 100 mg/L, a clear blue precipitate appeared at low Fe:CN^- molar ratio, showing that the precipitation of Prussian Blue was more favorable with high concentration of cyanide. At the Fe:CN^- molar ratio >1.2, the solution turned into a dark blue-brown color, indicating the excess of iron precipitated as ferric hydroxide. Although increasing Fe:CN^- molar ratio elevates the removal efficiency of CN^-, the purity of the Prussian Blue is greatly compromised.

Figure 6B showed the diffraction patterns of the precipitate, produced at initial CN^- concentration of 100 mg/L and the theoretical Fe:CN^- molar ratio of 0.5, indicating that PB was nearly the sole product generated. SEM-EDS results showed that the four major constituents, Fe, C, N and O, and the Fe:CN^- molar ratio in the precipitate is 0.21 (see Figure 6C). The ratio was a bit lower than the value expected for the Fe:CN^- molar ratio of PB (0.39), indicating that additional CN^- was removed by adsorption on iron hydroxides other than PB precipitation. Moreover, the precipitate was composed of 8 %wt of other components, mainly Na, Cl and K, due to the chemical for increasing the conductivity and impurities being released from the electrode.

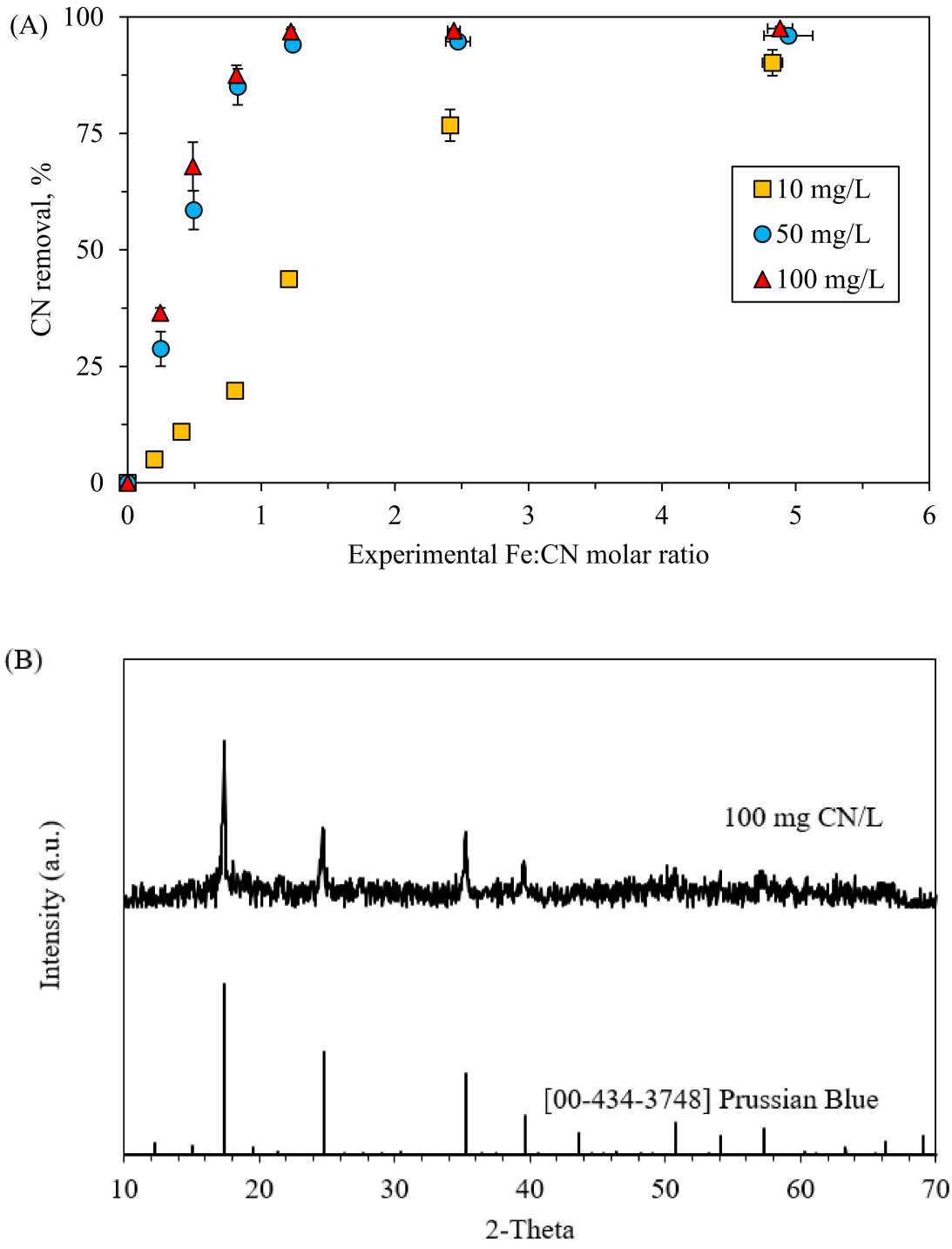

Figure 6. *Cont.*

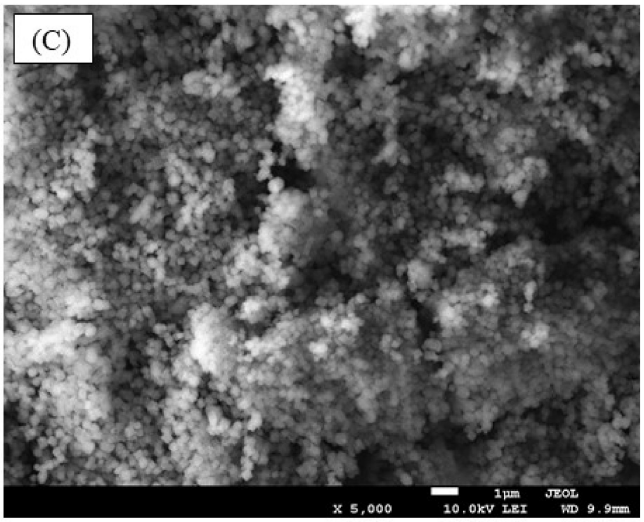

Item \ Sample	Initial concentration of 100 mg CN^-/L
Fe, atomic %	13.87
C, atomic %	39.39
N, atomic %	27.86
O, atomic %	14.18
Fe:CN^- molar ratio	0.21

Figure 6. (**A**) CN^- removal as a function of Fe:CN^- molar ratio for various initial concentration. (**B**) XRD powder pattern and (**C**) SEM observation of the precipitate produced at initial concentration of 100 mg CN^-/L and the theoretical Fe:CN^- molar ratio of 0.5. Control pH of 7. Current intensity of 1 A. Mechanical mixing.

3.5. Effects of DO

Three DO levels were investigated using aeration (initial DO of 8.3 mg O_2/L), stirring (initial DO of 5.1 mg O_2/L) and nitrogen purging (initial DO of 1.0 mg O_2/L). The experiments were performed at the control pH of 7 and initial CN^- concentration of 10 mg/L. As shown in Figure 7A, CN^- removal reached about 85% at the experimental Fe:CN^- molar ratio of 5.7 under the three DO conditions. However, CN^- removal increased faster under low DO conditions and the color of the solution remained blue under low to middle DO conditions. At the high DO level, the $Fe^{III}(CN)_6^{3-}$ complex is expected to be the dominant specie due to the conversion of Fe(II) to Fe(III) [19], but the brown/green color of the solution suggested ferric hydroxides precipitated too. Under a low DO level, $Fe^{II}(CN)_6^{4-}$ forms, then precipitates as $Fe^{II}_2Fe^{II}(CN)_{6(s)}$. According to Yu et al. (2016) [7], iron(II) ferrocyanide ($Fe^{II}_2Fe^{II}(CN)_{6(s)}$) is an intermediate in the formation of PB. As shown in Figure 7B, the XRD pattern of precipitate formed under low DO level showed a high noise level compared to the precipitate formed at middle DO level. Moreover, SEM observation showed square particles were formed under low DO level, instead of the accumulation of tiny circle particles under middle DO level (see Figure 7C,D). These results might be explained by the formation iron (II) ferrocyanide instead of PB. DO conditions did not greatly affect the removal of CN^- but did affect the quality of the recovery product. Extreme DO levels, such as high DO, which is favorable to the oxidation of ferrous to ferric, or low DO level, which is favorable to maintain ferrous in the system, are not optimal conditions for the precipitation of Prussian Blue. Prussian Blue is composed of ferrous and ferric ions, and it is preferable to form in the middle DO level.

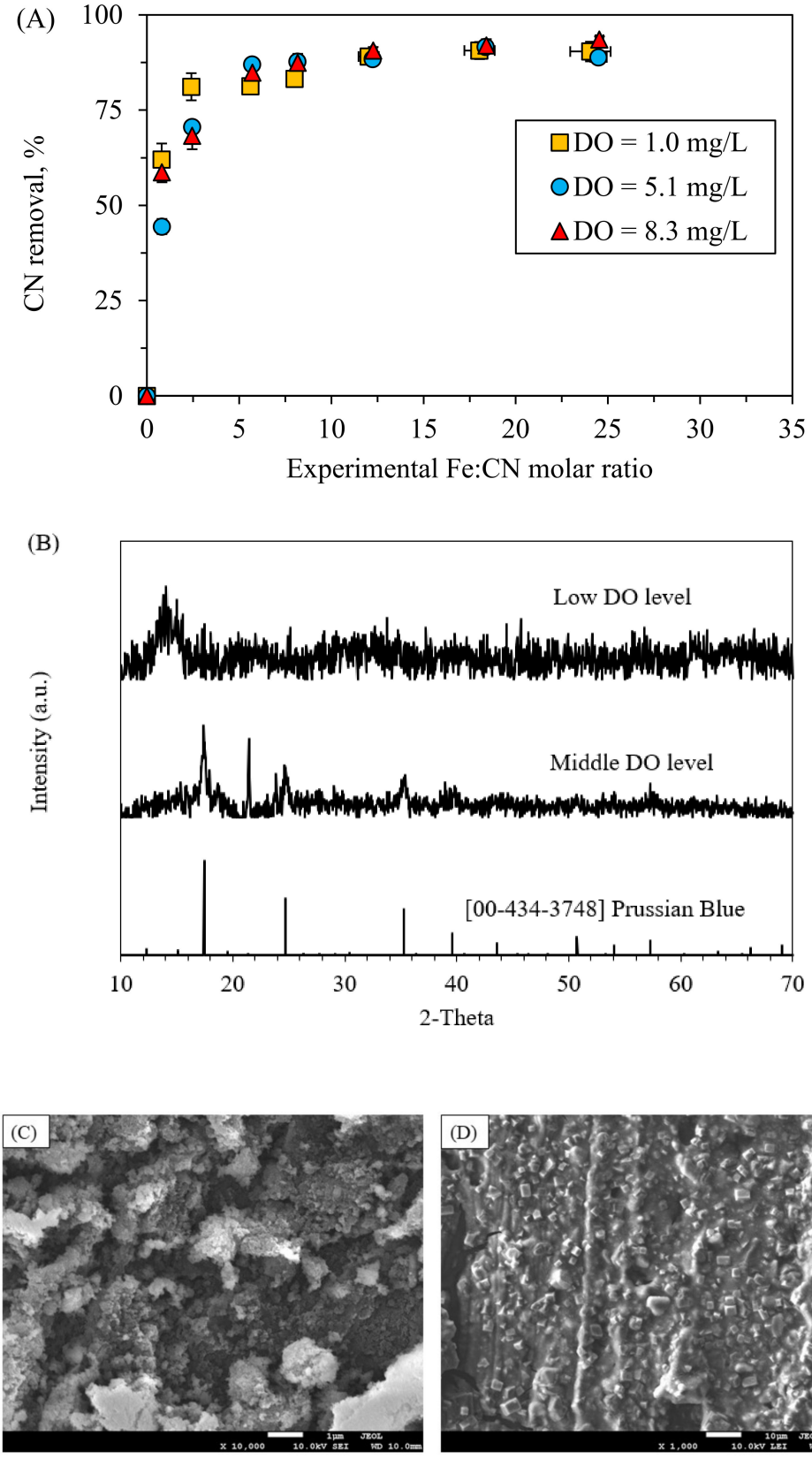

Figure 7. (**A**) CN^- removal as a function of the experimental Fe:CN^- molar ratio for various initial DO levels; (**B**) XRD powder patterns and (**C**) SEM observations of the precipitates produced at Fe:CN^- molar ratio of 0.8, (**C**) middle and (**D**) low DO levels. Initial CN^- concentration of 10 mg/L. Control pH of 7. Current intensity of 1 A.

3.6. Post Treatment to Achieve the Discharge Limit Requirement

Cyanide was recovered as PB under the optimal conditions of pH 7, Fe:CN^- molar ratio varying from 0.5 to 0.8 at middle DO level. At the Fe:CN^- molar ratio of 0.8, only 45%, 85% and 87.5% of cyanide was removed for initial CN^- concentrations of 10, 50 and 100 mg/L, respectively. The treated water did not meet the discharge limit of cyanide in Taiwan (1 mg CN^-/L). After recovery of PB by filtration, secondary treatment through the oxidation of cyanide using H_2O_2 under the initial pH of 7 and reaction time of 10 min was investigated. During this process, cyanide is oxidized as cyanate then further oxidized to ammonium and carbonate as shown in Equations (4) and (5) [20].

$$CN^- + H_2O_2 \rightarrow OCN^- + H_2O \quad (4)$$

$$OCN^- + 2H_2O \rightarrow NH_4^+ + CO_3^{2-}. \quad (5)$$

For an initial CN^- concentration of 10 mg/L, an overall removal of 87% and 92% of CN^-, corresponding to the final CN^- concentration of 1.3 and 0.8 mg/L, was achieved at the H_2O_2:CN molar ratio of 1:1 and 1.5:1, respectively. The values are 92 and 99% respectively at the H_2O_2: CN^- molar ratio of 1:1 and 1.5:1 for at the initial concentration of 100 mg CN^-/L, i.e., the final CN^- concentration of 8 and 1 mg/L, as shown in Figure 8. With the H_2O_2:CN molar ratio of 1.5:1, the discharge limit of 1 mg CN^-/L was reached for both initial CN^- conditions. Moreover, this method did not require the use of a catalyst because of the presence of dissolved Fe(II) ions in the solution. Fe(II) ions react easily with H_2O_2, what is known as the Fenton process, to degrade the contaminants. The reaction between Fe(II) ions and H_2O_2 might help to degrade iron cyanide complexes in solution. After H_2O_2 was added, the solution turned to orange and ferrous ions in the solution were oxidized into ferric ions and then precipitated as ferric hydroxides. The cost of this secondary process was calculated based on the redox reactions and the number of electrons needed to remove cyanide as shown in Equation (6).

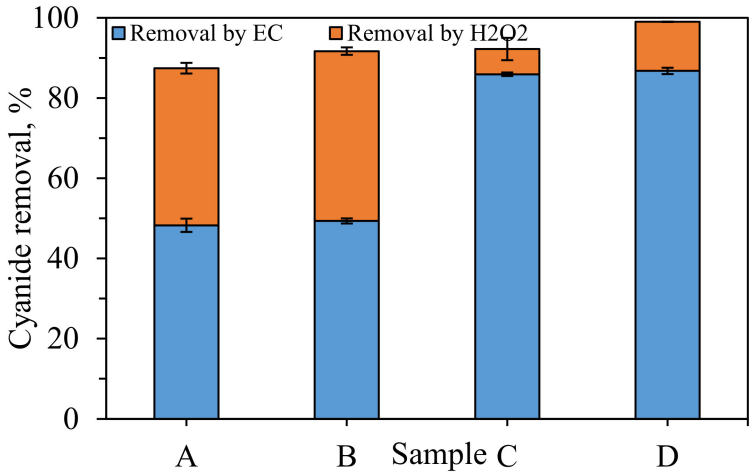

Figure 8. Removal of cyanide with electrochemical crystallization followed by oxidation of residual cyanide using H_2O_2. Sample A: initial concentration of 10 mg CN^-/L, H_2O_2:CN = 1:1. Sample B: initial concentration of 10 mg CN^-/L, H_2O_2:CN = 1.5:1. Sample C: initial concentration of 100 mg CN^-/L, H_2O_2:CN = 1:1. Sample D: initial concentration of 100 mg CN^-/L, H_2O_2:CN = 1.5:1. Reaction time of the secondary treatment is 10 min. Fe:CN^- molar ratio of 0.8 and pH of 7.

$$H_2O_2 + 2H^+ + 2e^- \rightarrow 2H_2O \quad (6)$$

The cost of H_2O_2 (purity, 30%) was estimated to be 0.35 USD/kg. The oxidation method by H_2O_2 had a lower cost (1.14 USD/kg CN^- with H_2O_2:CN^- molar ratio of 1.5:1) than alkaline chlorination, which costs around 9.7 USD/kg CN^-. The cost of electro-

chemical crystallization was also assessed, based on the method in Martin et al. [21]. Only 1.9 USD/kg CN^- for the electrochemical process was required to recover PB, leading to a total cost of the process of 3.04 USD/kg CN^-. Electrochemical crystallization process with polishing treatment can save approximately 68% of the operating cost for alkaline chlorination.

4. Conclusions

The removal and recovery of cyanide by electrochemical crystallization of Prussian Blue using iron electrode was studied on synthetic CN-rich water. Various parameters were investigated, such as Fe:CN^-, pH, DO level and initial CN^- concentration, and the process was completed by H_2O_2 oxidation to achieve the discharge limit. The following conclusion can be drawn.

1. Through the chemical equilibrium modeling, the optimal pH and Fe: CN^- molar ratio were obtained. Prussian Blue was best formed at the pH $\leq$ 7 and the Fe:CN^- molar ratio $\leq$ 1.5. The recovery rate of Prussian Blue should increase with increasing initial CN^- concentration.
2. The complexation of cyanide and iron prevented the vaporization of HCN at pH < 9.2. In contrast to alkaline chlorination, electrochemical crystallization process for CN^- removal does not require high chemical costs for alkaline pH control.
3. Cyanide was removed up to 45% at the Fe:CN^- molar ratio of 0.8, pH of 7 and under middle DO level for the initial CN^- concentration of 10 mg/L. Solid analysis showed the production of Prussian Blue in the pH range of 5–7.
4. CN^- removal increased with increasing initial CN^- concentration. Where 88% of removal was achieved for an initial CN^- concentration of 100 mg/L, only 20% of CN^- was removed at initial CN^- concentration of 10 mg/L for the same condition. Moreover, solid analysis revealed higher Prussian Blue quality with increasing initial CN^- concentration.
5. DO levels did not affect the cyanide removal. However, solid analysis showed a better quality of the recovery product under middle DO conditions.
6. Polishing treatment by H_2O_2 oxidation was necessary to reach the discharge limit of 1 mg CN^-/L with the H_2O_2:CN^- molar ratio of 1.5. The cost of the total process was accessed as 1.9 USD/kg CN^- treated for electrochemical process and 1.14 USD/kg CN^- treated for post treatment.
7. This process might be interesting for cyanide removal and recovery on rich cyanide electroplating wastewater, containing high concentrations of cyanide and heavy metals. However, other pollutants might interfere in the reaction between cyanide and iron. Further investigation might be done on industrial wastewater.

Supplementary Materials: The following are available online at https://www.mdpi.com/article/10.3390/w13192704/s1, Figure S1. Percentage of Fe(II) in $Fe(OH)_2$ as a function of Fe:CN^- molar ratio and pH modeled by a chemical equilibrium software, MINEQL+. Fixed CN^- concentration of 10 mg/L. Temperature of 25 °C. Figure S2. Percentage of Fe(III) in $Fe(OH)_3$ as a function of Fe:CN^- molar ratio and pH modeled by a chemical equilibrium software, MINEQL+. Fixed CN^- concentration of 10 mg/L. Temperature of 25 °C.

Author Contributions: Conceptualization, N.M. and C.-W.L.; methodology, N.M. and V.Y.; writing—original draft preparation, N.M.; writing—review and editing, C.-W.L., V.N. and K.-H.C.; supervision, C.-W.L.; project administration, C.-W.L.; funding acquisition, C.-W.L. All authors have read and agreed to the published version of the manuscript.

Funding: This research was founded by Ministry of Science and Technology, Taiwan, grant number 107-2221-E-032-001-MY3.

Institutional Review Board Statement: Not applicable.

Informed Consent Statement: Not applicable.

Data Availability Statement: Not applicable.

Acknowledgments: The study has been supported by the Ministry of Science and Technology of Taiwan under Grant Number 107-2221-E-032-001-M Y3.

Conflicts of Interest: The authors declare no conflict of interest.

References

1. Lin, M.; Gu, Q.; Cui, X.; Liu, X. Cyanide Containing Wastewater Treatment by Ozone Enhanced Catalytic Oxidation over Diatomite Catalysts. *MATEC Web Conf.* **2018**, *142*, 1003. [CrossRef]
2. Malinovic, B.N.N.; Djuricic, T.; Vucanovic, A. Influence of hydraulic retention time on cyanide removal by electrocoagulation process. *J. Environ. Prot. Ecol.* **2018**, *19*, 628–637.
3. Botz, M.M. Overview of cyanide treatment methods. *Gold Inst.* **1999**, *11*, 28–30.
4. Kuyucak, N.; Akcil, A. Cyanide and removal options from effluents in gold mining and metallurgical processes. *Miner. Eng.* **2013**, *50–51*, 13–29. [CrossRef]
5. Ghosh, R.S.; Dzombak, D.A.; Luthy, R.G. Equilibrium precipitation and dissolution of iron cyanide solids in water. *Environ. Eng. Sci.* **1999**, *16*, 293–313. [CrossRef]
6. Adams, M.D. The removal of cyanide from aqueous solution by the use of ferrous sulphate. *J. S. Afr. Inst. Min. Metall.* **1992**, *92*, 17–25.
7. Yu, X.; Xu, R.; Wei, C.; Wu, H. Removal of cyanide compounds from coking wastewater by ferrous sulfate: Improvement of biodegradability. *J. Hazard. Mater.* **2016**, *302*, 468–474. [CrossRef] [PubMed]
8. Chiang, Y.H. Research and Application of Prussian Blue in Modern Science. *IOP Conf. Ser. Earth Environ. Sci.* **2019**, *384*, 012005. [CrossRef]
9. Mamelkina, M.A.; Herraiz-Carboné, M.; Cotillas, S.; Lacasa, E.; Sáez, C.; Tuunila, R.; Sillanpää, M.; Häkkinen, A.; Rodrigo, M.A. Treatment of mining wastewater polluted with cyanide by coagulation processes: A mechanistic study. *Sep. Purif. Technol.* **2020**, *237*, 116345. [CrossRef]
10. Stumm, W. *Chemistry of the Solid-Water Interface: Processes at the Mineral-Water and Particle-Water Interface in Natural Systems*; Wiley-Interscience: New York, NY, USA, 1992.
11. Lakshmanan, D.; Clifford, D.A.; Samanta, G. Ferrous and Ferric Ion Generation During Iron Electrocoagulation. *Environ. Sci. Technol.* **2009**, *43*, 3853–3859. [CrossRef] [PubMed]
12. Meunier, N.; Drogui, P.; Montané, C.; Hausler, R.; Mercier, G.; Blais, J.F. Comparison between electrocoagulation and chemical precipitation for metals removal from acidic soil leachate. *J. Hazard. Mater.* **2006**, *137*, 581–590. [CrossRef] [PubMed]
13. Moussavi, G.; Majidi, F.; Farzadkia, M. The influence of operational parameters on elimination of cyanide from wastewater using the electrocoagulation process. *Desalination* **2011**, *280*, 127–133. [CrossRef]
14. Zhao, X.; Wang, H.; Chen, F.; Mao, R.; Liu, H.; Qu, J. Efficient treatment of an electroplating wastewater containing heavy metal ions, cyanide, and organics by H2O2 oxidation followed by the anodic Fenton process. *Water Sci. Technol.* **2013**, *68*, 1329–1335. [CrossRef] [PubMed]
15. Merzouk, B.; Gourich, B.; Sekki, A.; Madani, K.; Vial, C.; Barkaoui, M. Studies on the decolorization of textile dye wastewater by continuous electrocoagulation process. *Chem. Eng. J.* **2009**, *149*, 207–214. [CrossRef]
16. Elsahwi, E.S.; Hopp, C.E.; Dawson, F.P.; Ruda, H.E.; Kirk, D.W. Principles and Economic Considerations of Electrochemical Treatment of Cyanide-Laden Wastewater. *IEEE Trans. Ind. Appl.* **2019**, *55*, 3274–3286. [CrossRef]
17. APHA. *Standard Methods for the Examination of Water and Waste Water*, 21st ed.; American Public Health Association: Washington, DC, USA, 2005; ISBN 0875530478.
18. Gražulis, S.; Daškevič, A.; Merkys, A.; Chateigner, D.; Lutterotti, L.; Quirós, M.; Serebryanaya, N.R.; Moeck, P.; Downs, R.T.; Le Bail, A. Crystallography Open Database (COD): An open-access collection of crystal structures and platform for world-wide collaboration. *Nucleic Acids Res.* **2012**, *40*, 420–427. [CrossRef]
19. Chuang, S.-M.; Ya, V.; Feng, C.-L.; Lee, S.-J.; Choo, K.-H.; Li, C.-W. Electrochemical Cr(VI) reduction using a sacrificial Fe anode: Impacts of solution chemistry and stoichiometry. *Sep. Purif. Technol.* **2018**, *191*, 167–172. [CrossRef]
20. Sarla, M.; Pandit, M.; Tyagi, D.K.; Kapoor, J.C. Oxidation of cyanide in aqueous solution by chemical and photochemical process. *J. Hazard. Mater.* **2004**, *116*, 49–56. [CrossRef] [PubMed]
21. Martin, N.; Ya, V.; Leewiboonsilp, N.; Choo, K.-H.; Noophan, P.; Li, C.-W. Electrochemical crystallization for phosphate recovery from an electronic industry wastewater effluent using sacrificial iron anodes. *J. Clean. Prod.* **2020**, *276*, 124234. [CrossRef]